IEEE Access
Multidisciplinary | Rapid Review | Open Access Journal

Received February 22, 2021, accepted March 3, 2021, date of publication March 9, 2021, date of current version March 16, 2021.

Digital Object Identifier 10.1109/ACCESS.2021.3064584

Eigen-Structure Assignment-Based Differential Evolution Algorithm for T-S Fuzzy Control Tuning Applied to Water-Turbine Governing System

YIDONG ZOU[1], JING QIAN[1], YUN ZENG[1], YAQING GUO[1], MENGYUN WU[1], FANGFANG WANG[1], AND HONG MEI[2]

[1]Faculty of Metallurgical and Energy Engineering, Kunming University of Science and Technology, Kunming 650000, China
[2]City College, Kunming University of Science and Technology, Kunming 650093, China

Corresponding authors: Jing Qian (qj0117@163.com) and Yun Zeng (zengyun001@163.com)

This work was supported by the National Natural Science Foundation of China under Grant 51869007.

ABSTRACT In this paper, a novel Takagi-Sugeno (T-S) fuzzy controller based on eigenstructure assignment (EA) and optimized by differential evolution algorithm (DE) is proposed, and the application of this control strategy in the hydro-turbine governing system (HTGS) is studied. Based on the non-linear model of HTGS, the corresponding state-space equations (SSE) are obtained by linearization through multiple equilibrium points. Combining with the principle of T-S fuzzy control, a T-S fuzzy model of HTGS integrating multiple SSE with generator power angle as a prerequisite is established. This paper adopts the EA method to design the fitness function in the optimization process and uses DE to complete the optimization operation to improve the performance of T-S fuzzy control in HTGS. Which makes each Linear-Quadratic-Regulator (LQR) controller gain in the fuzzy control reach the optimal under the constraint conditions. The simulation results show that compared with the standard fitness functions IAE (integral absolute error), ITAE (integral time absolute error) and ISE (integral square error), the fitness function designed using the EA method can expand the angle between the left and right eigenvectors of the T-S closed-loop system, and push the closed-loop pole from the imaginary axis to the left. That will make the adjustment time of the system shorter and the robustness against external interferences enhanced. The results also show that the proposed control strategy has better dynamic performance during the non-linear motion of HTGS and is superior to the existing control strategy.

INDEX TERMS Hydro-turbine governing system, fuzzy control, linear-quadratic-regulator, differential evolution algorithm, controller optimization.

I. INTRODUCTION

The largest clean energy hydropower is one of the most important components in the power supply. In recent years, especially in China, it has been vigorously developed [1]. Worldwide, nearly one-fifth of the power supply comes from Hydropower energy [2]. The safety and stability of hydropower energy main equipment and HTGS also face many urgent problems [3], [4]. HTGS is a coupling non-minimum phase and the complex non-linear system as it is an integral of the hydraulic, mechanical, and electrical system [5], [6]. Whether HTGS has excellent performance is related to the hydro generator safe and stable operation and even the power grid [7]. The main task of HTGS is to control the power of the hydro-turbine to the grid and maintain the system frequency at the rated value. Therefore, the research on the stability and reliability of HTGS is of significance.

Given the non-linear HTGS model and control problems, related scholars have discussed several studies. In the non-linear modeling of HTGS, a non-linear differential algebraic model of a multi-turbine turbine with a multi-turbine and surge tank is constructed, which makes it easier to design and analyze the stability of the unit that takes into account hydraulic coupling [8]. Under different operating conditions of HTGS, a non-linear mathematical model of HTGS considering the fractional derivative and time delay and of HTGS

The associate editor coordinating the review of this manuscript and approving it for publication was Xujie Li.

during load rejection using non-linear dynamic transfer coefficients is established respectively [9], [10].

In the non-linear control of HTGS, PID control has become the main controller of this system due to its simple structure and easy implementation. Different intelligent optimization algorithms are used to optimize the parameters of the adjusted system controller under multiple goals to achieve the purpose of enhancing the performance of the PID controller [12]–[14]. Non-linear PID control, sliding mode control, model predictive control, Hamilton energy function method, and other non-linear control applications have been applied to HTGS control problems, and all have achieved good control effects [11], [15]–[17].

However, the non-linear modeling and control methods discussed above require a more in-depth mathematical foundation and are not easy to be mastered by most engineering and technical personnel.

In the field of control, T-S fuzzy control is a fairly classic method [18]. T-S fuzzy control basic idea is to linearize the non-linear model into a local state space under multiple specific regions and use fuzzy rules to synthesize these state spaces to replace the original non-linear system.

Practice and theory have proved that the T-S fuzzy model can approximate a non-linear system with arbitrary accuracy through local state information and fuzzy rules [19]. The nonlinear HTGS mathematical model is linearized and combined with appropriate fuzzy rules to construct a T-S fuzzy model, and the controller is designed on this basis. A T-S fuzzy controller based on the fractional-order system robust theory [20] and finite-time stability theory is designed, respectively [21]. As we all know, the nonlinear term in HTGS is mainly the power angle of the generator. However, the establishment of the T-S fuzzy model in [19]–[21] is based on the turbine speed as a prerequisite, and the physical meaning of the fuzzy model established in this way is not clear. In the process of system response, how the T-S fuzzy system fits the original nonlinear system is not discussed in detail and in-depth in these papers.

From the above discussion, we were motivated to present an optimal T-S fuzzy control based on the EA method fitness function and study the control strategy for the non-linear HTGS. The main contributions of this paper are reflected in the following: (1) the T-S fuzzy model of HTGS is established with generator power angle as the precondition; (2) the multiple LQR controllers are integrated into T-S fuzzy control under the parallel distributed compensation (PDC); (3) based on a special fitness function, the method of matrix eigenstructure assignment, these LQR controllers are optimized using optimization algorithms to improve the performance of T-S fuzzy control. (4) the fuzzy control obtained by the optimization solution is applied to the HTGS.

The remaining part of this paper is organized as follows. Section II introduces the T-S fuzzy model and its control. The HTGS fuzzy model with the power angle as the precondition is established in Section III. Section IV presents in detail the optimized process operation of the fitness function and optimization algorithm. The simulation research cases of HTGS under different disturbances are carried out and discuss experimental results in Section V. Finally, the conclusions are summarized in Section VI.

II. TAKAGI-SUGENO FUZZY SYSTEM

A. TAKAGI-SUGENO FUZZY MODEL

For a continuous non-linear system with n state variables and m control inputs, its T-S fuzzy model can be represented by the following r fuzzy rules.

rule R^i:If $x_1(t)$ is $\boldsymbol{M_1^i}$ and $x_2(t)$ is $\boldsymbol{M_2^i}\ldots$and $x_j(t)$ is $\boldsymbol{M_j^i} x_n(t)$ is $\boldsymbol{M_n^i}$

$$\text{Then } \dot{x}(t) = \boldsymbol{A_i} x(t) + \boldsymbol{B_i} u(t), \quad i = 1, 2, \ldots, r \tag{1}$$

where $\boldsymbol{M_j^i}$ is the j th membership function of the ith rule, the state vector $x(t) \in R^n$, $A_i \in R^{n\times n}$,$u(t)$ is the control input variable, R^i is the ith If-Then fuzzy rule.

Defined by the defuzzification of the fuzzy system, the overall output of the T-S fuzzy model formed by the fuzzy regular Eq. (1) can be expressed as

$$\dot{x} = \frac{\sum_{i=1}^{r} w_i(x(t))(\boldsymbol{A_i} x(t) + \boldsymbol{B_i} u(t))}{\sum_{i=1}^{r} w_i(x(t))} \tag{2}$$

where w_i is the output weight value of the membership function of ith rule of fuzzy model.

B. T-S FUZZY CONTROL

For each T-S fuzzy rule, the state feedback method is adopted to design r fuzzy control rules.

Control rules CR^i:

If $x_1(t)$ is $\boldsymbol{M_1^i}$ and $x_2(t)$ is $\boldsymbol{M_2^i}\ldots$and $x_j(t)$ is $\boldsymbol{M_j^i} x_n(t)$ is $\boldsymbol{M_n^i}$

$$\text{Then } u(t) = -\boldsymbol{K_i} x(t), \quad i = 1, 2, \ldots, r \tag{3}$$

where $\boldsymbol{K_i}$ is the ith state feedback control gain.

The Parallel Distributed Compensator (PDC) is a model-based model control designer method suitable for the non-linear system control problem of T-S fuzzy modeling. According to the definition of the anti-fuzzy system, for a continuous non-linear system, according to the PDC total, the control output can be expressed as:

$$u(t) = -\frac{\sum_{j=1}^{r} w_j(x(t))\boldsymbol{K_j} x(t)}{\sum_{j=1}^{r} w_j(x(t))} \tag{4}$$

where w_j is the output weight value of the membership function of jth rule of fuzzy control.

Refer to Eq. (2) and (4), the closed-loop T-S fuzzy system can be expressed as

$$\dot{x}(t) = \sum_{i=1}^{r} \sum_{j=1}^{r} w_i(x(t)) w_j(x(t)) [\boldsymbol{A_i} - \boldsymbol{B_i K_j}] x(t) \tag{5}$$

III. MATHEMATICAL MODEL OF HTGS

A. NON-LINEAR MATHEMATICAL MODEL OF HTGS

The dynamic characteristic of the synchronous generator could be presented as

$$\begin{cases} \dot{\delta} = \omega_0 \omega \\ \dot{\omega} = \dfrac{1}{H}\left(m_t - m_e - D\omega\right) \end{cases} \tag{6}$$

where δ is the generator rotor angle, D is the damping coefficient, ω is the generator rotor angular velocity, H is the generator rotor time constant, m_e is the electromagnetic torque, m_t is the main power torque of the turbine.

When the per-unit value is used, the following relationship exists between electromagnetic torque and electromagnetic power

$$m_e = P_e \tag{7}$$

The electromagnetic power of the salient-pole synchronous generator can be expressed as

$$P_e = \frac{E_q{}' V_s}{x_{d\sum}{}'} \sin\delta + \frac{V_s^2}{2} \frac{x_{d\sum}{}' - x_{q\sum}}{x_{d\sum}{}' x_{q\sum}} \sin 2\delta \tag{8}$$

where $E_q{}'$ is the transient internal voltage of the armature, V_s is the bus voltage at infinity, the direct axis transient reactance is $x_{d\sum}{}'$, the quadrature axis reactance is $x_{q\sum}$.

$x_{d\sum}{}'$ and $x_{q\sum}$ are expressed as

$$\begin{cases} x_{d\Sigma}{}' = x_d{}' + x_T + \dfrac{1}{2} x_L \\ x_{q\Sigma} = x_q + x_T + \dfrac{1}{2} x_L \end{cases} \tag{9}$$

where $x_d{}'$ and x_q are generator d-axis transient reactance and q-axis synchronous reactance respectively, x_T is the short-circuit reactance of the transformer, x_L is the reactance of the transmission line.

The differential equation of a hydraulic-servo system motion for controlling the opening of the guide vane of the water turbine given as

$$T_y \frac{dy}{dt} + y = u \tag{10}$$

where T_y is the time constant of the servomotor, y is the incremental deviation of the guide vane opening.

Considering that the turbine adopts the familiar, rigid water hammer model $G_h(s) = -T_w s$, the output torque of the turbine governing system is given as

$$\begin{cases} \dot{m}_t = \dfrac{1}{e_{qh} T_w} \left[-m_t + e_y y - \dfrac{e e_y T_w}{T_y} (u - y) \right] \\ e = \dfrac{e_{qh} e_h}{e_y} - e_{qh} \end{cases} \tag{11}$$

where e_{qh} is the transmission coefficient between the head and flow of the turbine, T_w is the hydraulic inertia time constant of the turbine, e_y is the transmission coefficient of the hydro-turbine servomotor stroke and the torque of the turbine, e_h is the transmission coefficient of the head and the torque of the turbine.

There is the following relationship between the main torque of the turbine and its power in per-unit value.

$$m_t = P_m \tag{12}$$

where P_m is the output power of the hydro-turbine.

According to Eq. (6)-(12), the mathematical model of HTGS can be described as:

$$\begin{cases} \dot{\delta} = \omega_0 \omega \\ \dot{\omega} = \dfrac{1}{H}\left(P_m - D\omega - \dfrac{E_q' V_s}{x_d'} sin\delta - \dfrac{V_s^2}{2} \dfrac{x_{d\Sigma}' - x_{q\Sigma}}{x_{d\Sigma}' x_{q\Sigma}} sin 2\delta\right) \\ \dot{P_m} = \dfrac{1}{e_{qh} T_w} \left[-P_m + e_y y - \dfrac{e e_y T_w}{T_y} (u - y) \right] \\ \dot{y} = \dfrac{1}{T_y}(u - y) \end{cases} \tag{13}$$

where u is the controller signal.

The relevant parameters of HTGS are shown in Appendix Table 1. The parameters in this part are the basis for the following T-S fuzzy model.

B. T-S FUZZT MODEL OF HTGS

For the non-linear HTGS described in equation (13), at a certain equilibrium state point, Jacobi is used to directly obtain the partial derivative method to obtain the corresponding state space

$$\dot{x}(t) = \boldsymbol{A} x(t) + \boldsymbol{B} u(t) \tag{14}$$

where $x = \begin{bmatrix} \delta & \omega P_m & y \end{bmatrix}^T$

$$\boldsymbol{A} = \begin{bmatrix} 0 & \omega_0 & 0 & 0 \\ -\dfrac{\boldsymbol{S_E'(\delta_i)}}{H} & -\dfrac{D}{H} & \dfrac{1}{H} & 0 \\ 0 & 0 & -\dfrac{2}{T_w} & \dfrac{2T_y + 2T_w}{T_w T_y} \\ 0 & 0 & 0 & -\dfrac{1}{T_y} \end{bmatrix}$$

$$\boldsymbol{B} = \begin{bmatrix} 0 & 0 & -\dfrac{2}{T_y} & \dfrac{1}{T_y} \end{bmatrix}^T$$

$$\boldsymbol{S_E'}(\boldsymbol{\delta_i}) = \frac{E_q' V_s}{x_d'} \cos(\delta_i) + V_s^2 \frac{x_{d\Sigma}' - x_{q\Sigma}}{x_{d\Sigma}' x_{q\Sigma}} \cos(2\delta_i)$$

From Eq. (13), it can be seen that the main non-linear term in the system is the generator power angle δ. The fuzzy set for this non-linear term is shown in Figs.1. The fuzzy sets M1-M8 represent the fuzzy rules $R^1 - R^8$ membership function.

It can be seen from Eq. (14) that S_E' after linearization processing will have different values at different equilibrium points. Therefore, the power angle δ is used as the precondition of the fuzzy rule to select different state spaces.

Select different generator power angles and obtain the $S_E'(\delta_i)$ values in different state spaces under the corresponding power angles. The different $S_E'(\delta_i)$ values obtained by combining the design of suitable T-S fuzzy rules are used. The approximation of a state-space equation to the non-linear mathematical model, the $S_E'(\delta)$ the numerical table is shown in TABLE 1.

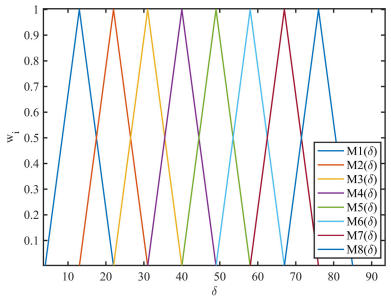

FIGURE 1. The membership function diagram in partial incremental form.

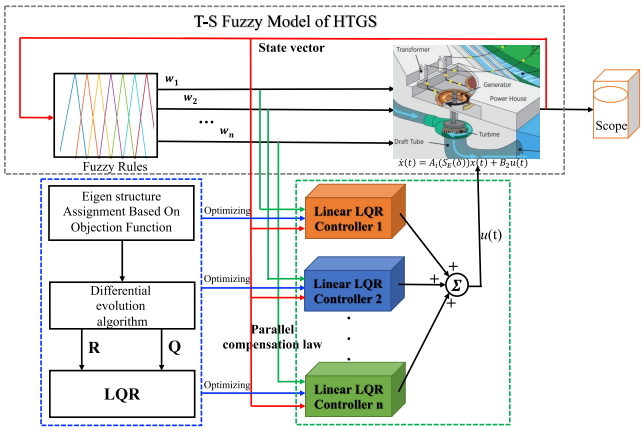

FIGURE 2. Structure of T-S control system of HTGS.

The $R^1 - R^8$ fuzzy rules designed in this paper are

$$R^i: \begin{cases} If\ \delta\ (t)\ is\ near\ \delta_i \\ Then\ \dot{x}\ (t) = \boldsymbol{A}\left(S'_E\ (\delta_i)\right) x\ (t) + \boldsymbol{B}u\ (t) \end{cases} \quad i = 1, 2 \ldots 8$$

The corresponding T-S fuzzy control rules are

$$R^i: \begin{cases} If\ \delta\ (t)\ is\ near\ \delta_i \\ Then\ u\ (t) = -\boldsymbol{K}_j x(t) \end{cases} \quad j = 1, 2 \ldots 8$$

Then, the closed-loop T-S fuzzy control system of HTGS governing system can be expressed as

$$\dot{x}(t) = \sum_{i=1}^{8} \sum_{j=1}^{8} w_i(\delta(t)) w_j(\delta(t))[\boldsymbol{A_i} - \boldsymbol{B_i K_j}] x(t) \quad (15)$$

IV. T-S FUZZY CONTROLLER OPTIMIZATION

According to HTGS closed-loop T-S fuzzy control system described in Eq. (15), the overall control system schematic diagram is shown in Figs. 2. The red dashed box is the T-S fuzzy model of HTGS, in which the black line outputs the value of w_i. The blue dashed box is the weighting matrix outputs under the optimization of the fitness function based on EA using DE. The green dashed box is the T-S fuzzy controller, where each part is the LQR controller, the red line is HTGS state feedbacks, and the green line output is the value of w_j. Each local LQR controller is summed by an adder and used as the T-S fuzzy controller overall output.

A. LINEAR-QUADRATIC-REGULATOR (LQR) CONTROLLER

As shown in Figs. 2, in the design of each local linear controller in T-S fuzzy control, this paper adopts the LQR control of state feedback. If the pair (A, B) are controllable, the LQR controller is used to find the feedback gain of the system. The minimization of the regulator includes the adjustment time response speed and the energy size of the state feedback control as the quadratic performance index below formula (16) to achieve the best control law u.

$$\boldsymbol{J} = \int_0^\infty \left(x^T \boldsymbol{Q} x + u^T \boldsymbol{R} u\right) dt \quad (16)$$

where $\boldsymbol{Q}$ is the weighting matrix of the state variables, $\boldsymbol{R}$ is the weighting matrix of the control variables.

The weighting matrix $\boldsymbol{Q}$ restricts the system state, and the weighting matrix $\boldsymbol{R}$ restricts the force exerted by the controller. The weight matrix $\boldsymbol{Q}$ and $\boldsymbol{R}$ are essentially adjustment variables that affect the performance of the controller. Generally speaking, $\boldsymbol{Q}$ is a symmetric positive definite matrix, and $\boldsymbol{R}$ is a symmetric positive definite matrix.

The optimal control law obtained by solving is

$$u\ (t) = -\boldsymbol{K} x(t) \quad (17)$$

$\boldsymbol{K}$ is the feedback gain of the closed-loop system, the calculation formula is

$$\boldsymbol{K} = -\boldsymbol{R}^{-1} \boldsymbol{B}^T \boldsymbol{P} \quad (18)$$

$\boldsymbol{P}$ is the solution of the given algebraic *Riccati* equation by

$$\boldsymbol{A}^T \boldsymbol{P} + \boldsymbol{P}\boldsymbol{A} - \boldsymbol{P}\boldsymbol{B}\boldsymbol{R}^{-1}\boldsymbol{B}^T \boldsymbol{P} + \boldsymbol{Q} = 0 \quad (19)$$

From the above discussion, it can be seen that the optimal control performance index depends on the selection of the constant weighting matrix. Therefore, the LQR optimization problem is transformed into optimally selecting the best weighting constant matrix $\boldsymbol{Q}$ and $\boldsymbol{R}$ so that the overall T-S fuzzy control design performance index can be met.

B. DIFFERENTIAL EVOLUTION ALGORITHM

DE has the characteristics of few undetermined parameters, not easy to fall into local optimum and fast convergence speed, and has become an effective method for solving nonlinear, multi-extreme, and multi-dimensional complex functions.

The steps of DE mainly include

Step 1: Generate the initial population. Generate population individuals that randomly meet the constraints in the n-dimensional space.

$$x_{ij}(0) = \mathrm{rand}_{ij}(0, 1)\left(x_{ij}^U - x_{ij}^L\right) + x_{ij}^L \quad (20)$$

where x_{ij}^U is the upper bound of the jth chromosome, x_{ij}^L is the lower bound of the jth chromosome, $rand_{ij}(0, 1)$ means generating a random number between (0,1).

Step 2: Randomly select several individuals x_{p1}, x_{p2} and x_{p3} from the current population, and then add the difference between any two individuals to the third individual after

scaling by the scaling factor F to obtain the target individual's mutation result. The process can be expressed as

$$h_{ij}(t+1) = x_{p1j}(t) + F\left(x_{p2j}(t) - x_{p3j}(t)\right) \tag{21}$$

Step 3: Crossover operation. The purpose of crossover operation is to increase the diversity of the population. Using the binomial crossover method, the operation process can be expressed as

$$v_{ij}(t+1) = \begin{cases} h_{ij}(t+1), & \text{rand } l_{ij}(0,1) \le CR \\ x_{ij}(t), & \text{rand } l_{ij}(0,1) > CR \end{cases} \tag{22}$$

where CR represents the crossover probability.

Step 4: Selection operation. The experimental vector generated after mutation and crossover will be competitively selected on the target vector to determine which vector is used for the next generation. The operation process is

$$x_i(t+1) = \begin{cases} v_i(t+1), & f\left(x_i^t\right) \le f\left(v_i^t\right) \\ x_{ij}(t), & f\left(x_i^t\right) > f\left(v_i^t\right) \end{cases} \tag{23}$$

where $f(\cdot)$ is the fitness function based on EA method. The discussion of the respective fitness functions will be discussed in the next section.

From **Step 1** to **Step 4**, it is not difficult to find that the standard DE searchability depends on the parameters. The parameter settings in the standard DE mainly include:

Population size. The population size chooses M_G as a fixed value, and the selection range is generally [20,50]. The larger the population size, the greater the probability of obtaining the optimal solution, but the solution time increases.

The number of iterations. The greater the maximum number of iterations, the greater the G_T, the more accurate the optimal solution. The greater the value of M_G and G_T will cause the calculation time of the algorithm to become longer.

Mutation factor. The mutation factor is an important parameter that determines population diversity and algorithm convergence speed, usually in the range of [0.3, 0.6]. To improve the convergence efficiency, a dynamic strategy to adjust the mutation factor F *is* adopted in this paper, and the adjustment strategy is as follows Eq. (24) as shown.

$$F = (F_{max} - F_{min})\frac{iter_{max} - iter}{\text{iter}_{max}} + F_{min} \tag{24}$$

where F_{max} is the maximum value of the set variation factor, F_{min} is the minimum value of the set variation factor, $iter_{max}$ is the maximum number of iterations; iter current iteration number.

Crossover factor (CR). CR determines the degree of crossover of the population. The smaller the CR, the smaller the population diversity. The larger the CR, the greater the population diversity, which will cause the algorithm to converge too slowly, usually a fixed value [0.6, 0.9]. To ensure the diversity of the population and improve the convergence speed of the algorithm, the dynamic adjustment strategy of CR is expressed as.

$$CR = (CR_{max} - CR_{min})\frac{iter}{iter_{max}} + CR_{min} \tag{25}$$

where CR_{max} is the maximum value of CR, CR_{min} is the minimum value of CR.

C. FITNESS FUNCTION BASED ON EIGEN-STRUCTUE ASSIGNMENT

To properly adjust the controller in the time domain and evaluate its performance, there are some performance standards in the time domain, and generally use standard fitness functions such as IAE, ITAE, ISE, etc. [25], [26].

The integral absolute error (IAE) is defined as the integral of the absolute value of the error, and its mathematical expression is

$$IAE = \int_0^\infty |e(t)|\, dt \tag{26}$$

The integral time absolute error (ITAE) is defined as the integral of absolute error multiplied by the change of time with time and its mathematical expression is

$$ITAE = \int_0^\infty |e(t)|\, t dt \tag{27}$$

The integral square error (ISE) is defined as the square integral mathematics of absolute error, and its mathematical expression is

$$ISE = \int_0^\infty |e(t)|^2\, dt \tag{28}$$

where e(t) is the control error.

The eigenstructure assignment (EA) method to design the fitness function was adopted to optimize and improve the performance of the LQR controller and achieved good control effects [29], [30]. Therefore, this paper uses the method to construct a fitness function. The structure of a matrix can be eigenvalue and eigenvector representation. The relationship between the associated matrix $\boldsymbol{A}$ in each SSE in the T-S fuzzy model described in Eq. (14) and its left and right eigenvalues is

$$\boldsymbol{A}\vec{v}_i = \lambda_i \vec{v}_i \tag{29}$$

$$\vec{w}_i^T \boldsymbol{A} = \lambda_i \vec{w}_i^T \tag{30}$$

where $\vec{v}_i$ is the right eigenvector, $\vec{w}$ is the left eigenvector, λ is the eigenvalue of matrix $\boldsymbol{A}$.

The relationship between the system control performance and the eigenvalues and eigenvectors of the closed-loop feedback system was pointed out [23]. (1) The system eigenvalue affects the speed of dynamic response; (2) the closed eigenvector affects the system control response shape. Then the system response can be expressed as

$$y(t) = \boldsymbol{C}\sum_{i=1}^{n} \vec{v}_i e^{\lambda_i t}\vec{w}_i^T x(0) + \sum_{i=1}^{n} \vec{v}_i \vec{w}_i^T \int_0^t \boldsymbol{C} e^{\lambda_i (t-\tau)} \boldsymbol{B} u(\tau) d\tau \tag{31}$$

where $x(0)$ is the initial state of the system, $\boldsymbol{B}$ and $\boldsymbol{C}$ are the state space matrix.

Therefore, Eq. (31) expresses the relationship between the time response and transient response generated by each

state space in the T-S fuzzy model and its eigenvalues and eigenvectors.

The distribution method of feature vectors is realized by finding the left and right feature vectors of the closed-loop feedback system. The right feature structure allocation can solve the problems of suppressing the vibration of the flexible structure and solving the problems of interference decoupling, and the left feature structure allocation is used to define controllability methods and other issues [24]. The sensitivity of a symmetric matrix to parameter disturbances is related to its eigenvector matrix [25].

The differential change of Eq. (29) is

$$d\boldsymbol{A}\vec{v}_i + \boldsymbol{A}d\vec{v}_i = d\lambda_i\vec{v}_i + \lambda_i d\vec{v}_i \tag{32}$$

$d\lambda_i$ can be obtained as

$$d\lambda_i = \left(d\boldsymbol{A}\vec{v}_i + \boldsymbol{A}d\vec{v}_i - \lambda_i d\vec{v}_i\right)\vec{v}_i^{-1} \tag{33}$$

By multiplying Eq. (33) up and down by $\vec{w}_i^T$, the eigenvalue differential change can be obtained as

$$d\lambda_i = \frac{\vec{w}_i^T d\boldsymbol{A}\vec{v}_i}{\vec{w}_i^T\vec{v}_i} \tag{34}$$

The differential change of the corresponding eigenvector is

$$d\vec{v}_i = \sum\nolimits_{j=1}^{n} d_{ij}\vec{v}_i \tag{35}$$

where d_{ij} is

$$\begin{cases} d_{ij} = \dfrac{\vec{w}_i^T d\boldsymbol{A}\vec{v}_i}{\left(\lambda_i - \lambda_j\right)\left(\vec{w}_i^T\vec{v}_i\right)} & (i \neq j) \\ d_{ij} = 0 & (i = j) \end{cases}$$

According to Eq. (34) and (35), the norming, both sides of the equation can be:

$$||d\lambda_i|| \leq \frac{\parallel d\boldsymbol{A} \parallel_2 ||\vec{w}_i||_2||\vec{v}_i||_2}{\left|\vec{w}_i^T\vec{v}_i\right|} = k_i \parallel d\boldsymbol{A} \parallel_2 \tag{36}$$

where $\|\|_2$ is the L2 norm of the feature vector, $k_i \in (1, \infty)$.

Define the condition number of λ_i as

$$k_i = \frac{||\vec{w}_i||_2||\vec{v}_i||_2}{\left|\vec{w}_i^T\vec{v}_i\right|} \tag{37}$$

The condition number defined by Eq. (37) characterizes the degree of sensitivity between the change of the eigenvalue λ and the system disturbance and uncertainty. The eigenstructure assignment robustness is the insensitivity relationship between the closed-loop eigenvalue and the system disturbance.

It is found from Eq. (37) that a small disturbance of O(e) in A will cause a small disturbance of the eigenvalue λ_i to be $O(e/|Cos\theta|)$.Therefore, when the left and right eigenvectors are orthogonal, the eigenvalue will be changed.

DE is used to search and select the upper and lower bounds of $\boldsymbol{Q}$ and $\boldsymbol{R}$ to complete the solution of the Riccati equation of formula (19) to find the state feedback gain $\boldsymbol{K}$. The corresponding closed-loop system $\dot{x} = (\boldsymbol{A} - \boldsymbol{BK})\,x$ is formed by the feedback gain $\boldsymbol{K}$. Different closed-loop gains will find different pole positions, then the cosine of the angle between the left and right eigenvectors of the eigenvalue is shown in Eq. (38).

$$\boldsymbol{N} = \frac{\boldsymbol{W}^T\boldsymbol{V}}{\parallel \boldsymbol{W} \parallel_2 \parallel \boldsymbol{V} \parallel_2} \tag{38}$$

where $\boldsymbol{W}$ and $\boldsymbol{V}$ are the sets of left and right feature vectors respectively, namely

$$\begin{cases} \boldsymbol{V} = \left[\vec{v}_i\right] = [v_1, v_2, \ldots, v_n] \\ \boldsymbol{W} = \left[\vec{w}_i\right] = [w_1, w_2, \ldots, w_n] \end{cases}$$

Since the MIMO system has multiple eigenvalues. Therefore, multiple eigenvectors, the fitness function is:

$$\min S = ||\sum \boldsymbol{N}_i|| \tag{39}$$

where S is the sum of the cosines of the angles between the left and right eigenvectors.

The left and right eigenvectors are orthogonal, which will cause the disturbance of the closed-loop eigenvalues so that the poles of the closed-loop system are well separated, and the left half of the complex plane moves. With the iteration of the DE, the algorithm converges in one direction. In this solution process, the left half of the complex plane within the upper limit of the eigenvalue sensitivity is separated, but it is far from the ring pole. Therefore, compared with the previous optimization iteration, the system will become less sensitive to disturbances, improving system stability, and robustness. The algorithm will stop after the iteration termination condition is met, and the obtained individual will give the minimum value of the cost fitness function. At this time, the $\boldsymbol{Q}$ and $\boldsymbol{R}$ matrices in a local LQR controller in the T-S fuzzy controller are the optimal weight matrices.

V. MENTS AND ANALYSIS OF THE RESULTS

A. CONTROLLER PERFORMANCE VERIFICATION

The simulation experiment process is completed in the MATLAB/Simulink environment, including the calculation of the weight matrix $\boldsymbol{Q}$ and $\boldsymbol{R}$ in the LQR and the construction of the T-S fuzzy model and control.

DE is used to optimize each LQR state feedback gain in the T-S fuzzy controller under the fitness function designed by the EA method. According to the previously discussed content, there are 8 LQR controllers corresponding to 8 local state spaces that need to be designed, and then integrated into T-S fuzzy control through PDC and fuzzy rules.

Figs. 3-10 is the process curve of optimization solution under $S_e'(13°) - S_e'(76°)$ state space. Table 2 lists the relevant parameters in DE. The calculation results are compared with genetic algorithm (GA), particle swarm optimization algorithm (PSO), and the comparison result is shown in Figs. 3-10.

It can be seen from Figs. 3-10 that after 100 generations of iterative calculations, DE can be close to convergence about the 10th or 30th time. The convergence time of PSO and GA far exceeds that of DE. At the same time, it can

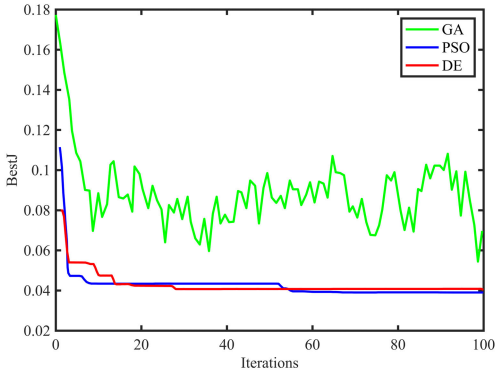

FIGURE 3. Algorithm convergence curve on $S_e'(13^\circ)$.

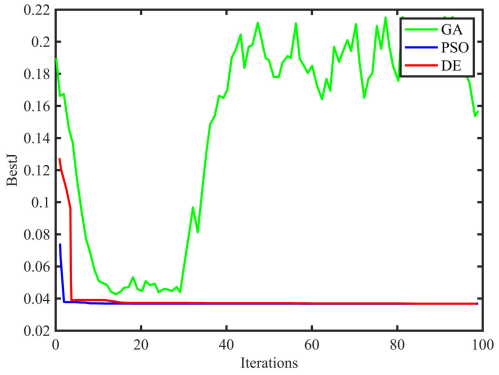

FIGURE 4. Algorithm convergence curve on $S_e'(22^\circ)$.

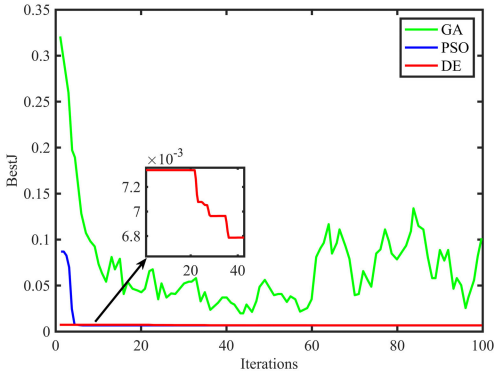

FIGURE 5. Algorithm convergence curve on $S_e'(31^\circ)$.

be seen from these figures that DE can better find the best value in each LQR. The use of both PSO and GA may cause the solution process to fall into a local optimal solution, especially GA cannot complete the convergence after 100 iterations. Therefore, it can be considered that the selected DE has higher efficiency and more accurate calculation results.

The results of the 8 weight matrices $\boldsymbol{Q}$ and $\boldsymbol{R}$ obtained after iterative optimization are as follows

$$\boldsymbol{Q}_1 = \begin{bmatrix} 100 & 0 & 0 & 0 \\ 0 & 100 & 0 & 0 \\ 0 & 0 & 1 & 0 \\ 0 & 0 & 0 & 1 \end{bmatrix}; \boldsymbol{R}_1 = 0.1;$$
$$\boldsymbol{Q}_4 = \boldsymbol{Q}_3 = \boldsymbol{Q}_2 = \boldsymbol{Q}_1;$$
$$\boldsymbol{R}_4 = \boldsymbol{R}_3 = \boldsymbol{R}_2 = \boldsymbol{R}_1.$$

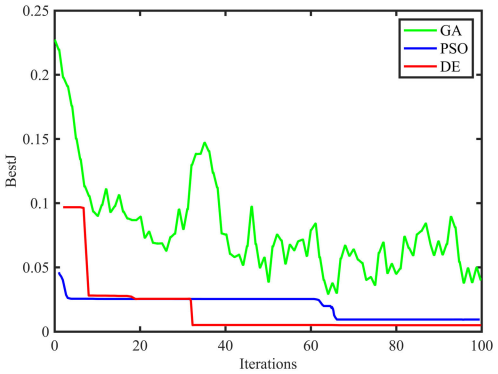

FIGURE 6. Algorithm convergence curve on $S_e'(40^\circ)$.

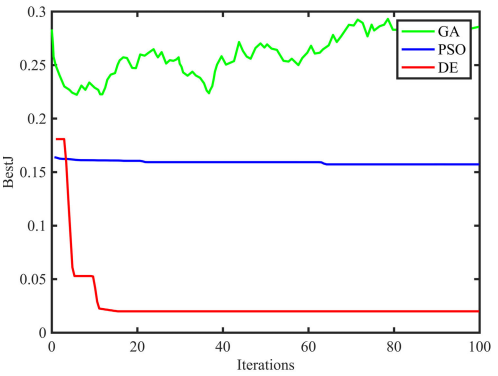

FIGURE 7. Algorithm convergence curve on $S_e'(49^\circ)$.

$$\boldsymbol{Q}_5 = \begin{bmatrix} 78.53 & 0 & 0 & 0 \\ 0 & 396.2020 & 0 & 0 \\ 0 & 0 & 1.0174 & 0 \\ 0 & 0 & 0 & 2.4748 \end{bmatrix};$$
$$\boldsymbol{R}_5 = 0.0068;$$
$$\boldsymbol{Q}_6 = \begin{bmatrix} 48.216 & 0 & 0 & 0 \\ 0 & 230.5023 & 0 & 0 \\ 0 & 0 & 1.0182 & 0 \\ 0 & 0 & 0 & 9.9641 \end{bmatrix};$$
$$\boldsymbol{R}_6 = 0.0337;$$
$$\boldsymbol{Q}_7 = \begin{bmatrix} 3.0082 & 0 & 0 & 0 \\ 0 & 398.1933 & 0 & 0 \\ 0 & 0 & 1.2018 & 0 \\ 0 & 0 & 0 & 1 \end{bmatrix};$$
$$\boldsymbol{R}_7 = 0.0968;$$
$$\boldsymbol{Q}_8 = \begin{bmatrix} 100 & 0 & 0 & 0 \\ 0 & 398.5792 & 0 & 0 \\ 0 & 0 & 1 & 0 \\ 0 & 0 & 0 & 1.0011 \end{bmatrix};$$
$$\boldsymbol{R}_8 = 0.0028;$$

Incorporating the eight weighting matrices $\boldsymbol{Q}_1 \sim \boldsymbol{Q}_8$ and $\boldsymbol{R}_1 \sim \boldsymbol{R}_8$ into the *Riccat* equation of the corresponding LQR, the state feedback gains $\boldsymbol{K}_1 \sim \boldsymbol{K}_8$ of the eight LQR controllers in the T-S fuzzy control can be obtained, which

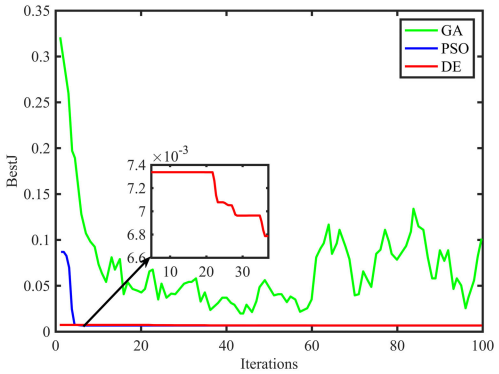

FIGURE 8. Algorithm convergence curve on S_{e1}'(58°).

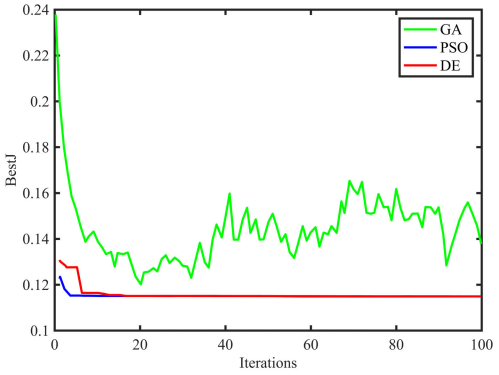

FIGURE 9. Algorithm convergence curve on S_{e1}'(67°).

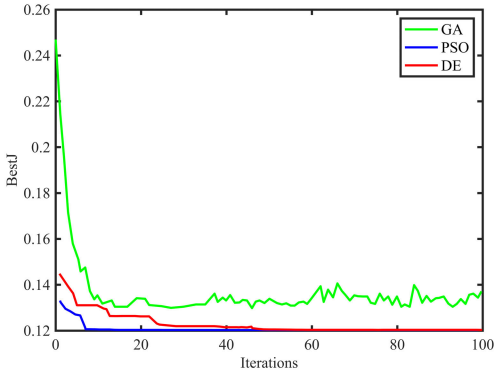

FIGURE 10. Algorithm convergence curve on S_{e1}'(76°).

are:

$$\begin{aligned}
\boldsymbol{K}_1 &= [-30.235 \quad -360.890 \quad 12.7065 \quad 33.691] \\
\boldsymbol{K}_2 &= [-30.453 \quad -325.425 \quad 13.9017 \quad 36.093] \\
\boldsymbol{K}_3 &= [-30.723 \quad -263.108 \quad 15.9577 \quad 40.222] \\
\boldsymbol{K}_4 &= [-30.954 \quad -157.914 \quad 19.3422 \quad 47.013] \\
\boldsymbol{K}_5 &= [-105.234 \quad 62.7002 \quad 84.8647 \quad 201.708] \\
\boldsymbol{K}_6 &= [-36.737 \quad 45.884 \quad 39.6371 \quad 100.072] \\
\boldsymbol{K}_7 &= [-5.351 \quad 16.0245 \quad 8.5366 \quad 24.6493] \\
\boldsymbol{K}_8 &= 10^3 \times [-0.0095 \quad 2.2649 \quad 0.0806 \quad 0.1655]
\end{aligned}$$

B. SIMULATION ANALYSIS

The simulations shown in this paper assume that the entire HTGS is in a stable state before 1 second. As shown in Figs. 11 and Figs. 12, the dynamic response curve of the system power angle and speed and the output curve of different fuzzy membership functions of HTGS under small disturbance conditions.

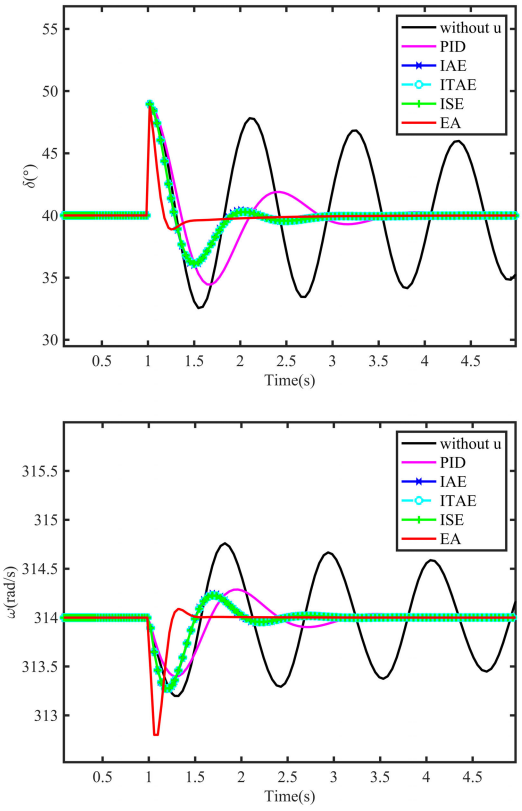

FIGURE 11. Dynamic performance of the power angle and speed of HTGS under small disturbances.

In this simulation, the machine power angle δ changes from 40° to 49°, and the power angle change rate $\Delta\delta$ is 9°. The red line in the figure represents the T-S fuzzy controller simulation waveform optimized and designed based on the EA method under this working condition. The blue line, bright blue line, and green line represent the T-S fuzzy controller simulation waveform based on the IAE, ITAE, and ISE methods. The pink line is the response curve of the controller designed by the traditional PID control method.

From the comparison results of these waveforms, the T-S fuzzy controller based on the EA fitness function optimization design in this paper can effectively make the system stable quickly, and the stabilization time is within 1 second. The control effect is significantly better than the optimization design based on its and the traditional fitness function. It is noted that the three fitness functions based on IAE, ITAE, and ISE method have not significantly improved the performance of the T-S fuzzy controller.

In this paper, the triangular membership function is used to realize the generator power angle fuzzification to complete the fitting of multiple linear state spaces to the non-linear mathematical model of HTGS. Eight fuzzy rules are used to realize this fuzzification. Figs. 12 shows the changes in the output weight value of the membership function under

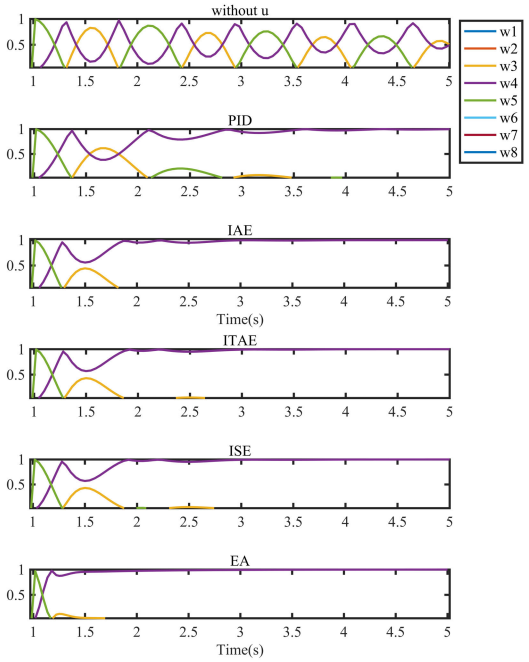

FIGURE 12. Changes in the membership weights of large disturbances.

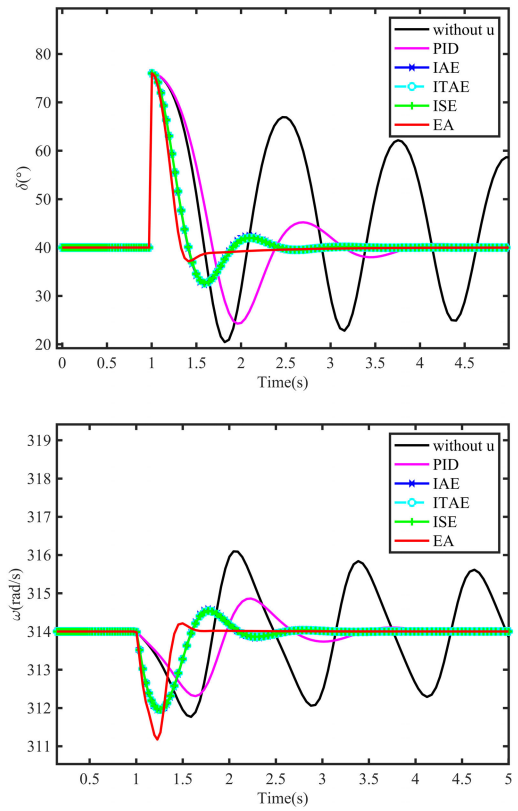

FIGURE 13. Dynamic performance of the power angle and speed ofHTGS under large disturbances.

different methods, where w_i is the output weight-value of the membership function of rule i.

It can be seen from the figure that the controller designed by the EA method can make the T-S fuzzy model of the HTGS stable in the $S'_e(40°)$ state within 1 second. The T-S fuzzy

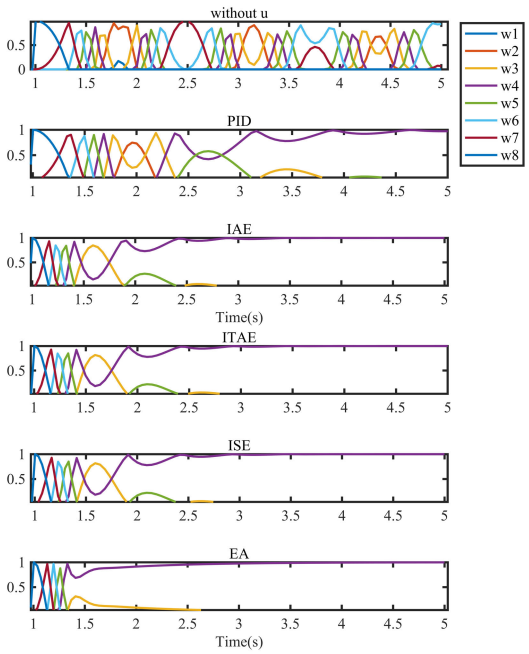

FIGURE 14. Changes in the membership weights of large disturbances.

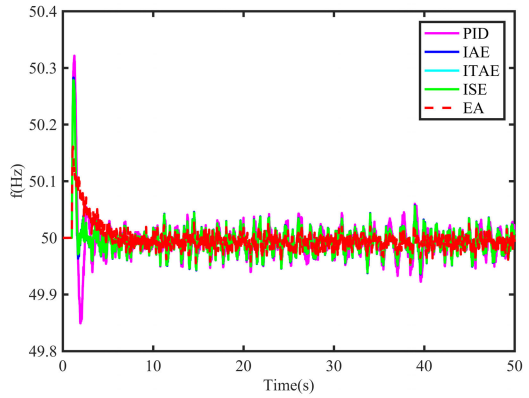

FIGURE 15. Dynamic performance of system frequency with the introduction of new energy power fluctuations.

controller designed based on the IAE, ITAE, and ISE methods has little difference in the fuzzy system from the figure weight value changes.

The simulation assumes that a three-phase short circuit occurs at the outlet of HTGS at t = 1s, the fault duration is 0.1s, and then the automatic reclosing quickly restores the fault line. The power angle and speed response of HTGS under this working condition is shown in Figs. 13.

The simulation results show that when a three-phase short-circuit accident occurs in the system, the system power angle and frequency recovery is very slow when the governing system adopts the traditional PID controller. However, the T-S fuzzy controller optimized based on various fitness functions has a stronger damping effect on the power angle, and the frequency oscillation time is shortened. As can be seen from the figure, the optimized design based on the EA method shows better performance than other optimized fitness in terms of adjusting time performance.

Figs.14 shows the change of each membership function output weight value under large disturbance conditions, and the curve change process reflects the switching process of each state space in the fuzzy system under the action of different T-S fuzzy controllers under this condition. T-S fuzzy model by switching between different states, the corresponding non-linear dynamic process can be fitted.

It can be seen from the figs. 14 that the optimization of T-S fuzzy controllers by ITA, ITAE, and ISE is not much different. Compared with no control strategy, the PID controller can stabilize the system in about 2.5 seconds, while ITA, ITAE, ISE, and optimized T-S The fuzzy controller basically stabilizes the system in 1.5 seconds, and it only takes about 1 second to complete the entire stabilization process using the EA method.

With the rapid development of more and more new energy sources such as wind power and photovoltaic power generation, this makes the robustness requirements of HTGS higher and higher.

Figs.15 simulates the introduction of a new energy power disturbance of 0.01±0.005pu in 1 second. From the simulation results under the same disturbance, the maximum system frequency is under the control of the controller optimized by the EA fitness function 50.15 Hz. The maximum frequency of the system under the optimally designed controller using IAE, ITAE, and ISE fitness functions has reached 50.28 Hz. The maximum frequency of the system under the control of the PID controller reaches 50.33Hz.

It can be seen from the figure that the frequency fluctuation range of the controller designed based on the EA method is smaller than that of other controllers. Therefore, the T-S fuzzy controller optimized by the EA method can improve the robustness of HTGS.

VI. CONCLUSION

In this paper, through the fitness function based on the EA method, DE is implemented based on the HTGS T-S fuzzy model to optimize the state feedback gain of each LQR under PDC, and the following conclusions are obtained: (1)Taking the generator power angle as the prerequisite, the nonlinear HTGS is linearized in the steady-state to obtain its state space method and combine the T-S fuzzy rules to complete the establishment of HTGS T-S fuzzy model; (2) To achieve the goal of comprehensive optimization of T-S fuzzy control of HTGS, each linear controller under fuzzy control is converted into an LQR optimization problem, and DE is used to obtain the minimized cost function to complete solving state feedback gain; (3) In the optimization process, the convergence process of different optimization algorithms is compared. DE shows better performance in terms of less convergence algebra and avoiding falling into local optimal solutions; (4) The simulation results show that based on the orthogonality between the left and right eigenvectors of an LTI system matrix, a fitness function is proposed and optimized to obtain the T-S fuzzy controller, which is better than the common IAE, ITAE and ISE standard fitness functions. The controller that comes out shows a shorter adjustment time, better transient performance, and stronger robust performance.

APPENDIX

TABLE 1. S_E'**-value table.**

power angle δ_i	13°(i=1)	22°(i=2)	31°(i=3)	40°(i=4)
$S_E'(\delta_i)$/H	-0.1462	-0.1362	-0.1218	-0.1036
power angle δ_i	49°(i=5)	58°(i=6)	67°(i=7)	76°(i=8)
$S_E'(\delta_i)$/H	-0.0826	-0.0598	-0.0362	-0.0128

TABLE 2. **Related parameters of algorithm.**

D_d	M_G	G_T	F_{max}	F_{min}	CR_{min}	CR_{max}	$iter_{max}$
7	50	100	0.7	0.2	0.5	0.1	100

TABLE 3. **Related parameters of HTGS.**

Symbol	Value	Symbol	Value
ω_0(rad/s)	314	D	2
H(sec)	9	E_q'	1.3
T_y(sec)	0.1	$x_{d\Sigma}'$	1.15
T_w(sec)	0.8	$x_{q\Sigma}$	1.474
V_s	1	e_{qh}	0.5
e	1	e_y	1.0

REFERENCES

[1] X. Sun, X. Wang, L. Liu, and R. Fu, "Development and present situation of hydropower in China," *Water Policy*, vol. 21, no. 3, pp. 565–581, Jun. 2019.

[2] G. Shahgholian, "An overview of hydroelectric power plant: Operation, modeling, and control," *J. Renew. Energy Environ.*, vol. 7, no. 3, pp. 14–28, 2020.

[3] B. Xu, H.-B. Jun, D. Chen, H. Li, J. Zhang, C. J. C. Blanco, and H. Shen, "Stability analysis of a hydro-turbine governing system considering inner energy losses," *Renew. Energy*, vol. 134, pp. 258–266, Apr. 2019.

[4] H. Li, B. Xu, E. Arzaghi, R. Abbassi, D. Chen, G. A. Aggidis, J. Zhang, and E. Patelli, "Transient safety assessment and risk mitigation of a hydroelectric generation system," *Energy*, vol. 196, Apr. 2020, Art. no. 117135.

[5] J. Yang, M. Wang, C. Wang, and W. Guo, "Linear modeling and regulation quality analysis for hydro-turbine governing system with an open tailrace channel," *Energies*, vol. 8, no. 10, pp. 11702–11717, Oct. 2015.

[6] W. Guo, J. Yang, M. Wang, and X. Lai, "Nonlinear modeling and stability analysis of hydro-turbine governing system with sloping ceiling tailrace tunnel under load disturbance," *Energy Convers. Manage.*, vol. 106, pp. 127–138, Dec. 2015.

[7] C. Li, L. Chang, Z. Huang, Y. Liu, and N. Zhang, "Parameter identification of a nonlinear model of hydraulic turbine governing system with an elastic water hammer based on a modified gravitational search algorithm," *Eng. Appl. Artif. Intell.*, vol. 50, pp. 177–191, Apr. 2016.

[8] Q. Jing, Z. Yun, L. Shunli, and G. Yakun, "Multi-machine differential-algebraic model of hydraulic turbine with complex hydraulic system," *Proc. Chin. Soc. Elect. Eng.*, vol. 40, no. 2, pp. 615–623, 2020.

[9] F. Wang, D. Chen, B. Xu, and H. Zhang, "Nonlinear dynamics of a novel fractional-order Francis hydro-turbine governing system with time delay," *Chaos, Solitons Fractals*, vol. 91, pp. 329–338, Oct. 2016.

[10] H. Zhang, D. Chen, B. Xu, and F. Wang, "Nonlinear modeling and dynamic analysis of hydro-turbine governing system in the process of load rejection transient," *Energy Convers. Manage.*, vol. 90, pp. 128–137, Jan. 2015.

[11] S. Huang, B. Zhou, S. Bu, C. Li, C. Zhang, H. Wang, and T. Wang, "Robust fixed-time sliding mode control for fractional-order nonlinear hydro-turbine governing system," *Renew. Energy*, vol. 139, pp. 447–458, Aug. 2019.

[12] X. Lai, C. Li, J. Zhou, Y. Zhang, and Y. Li, "A multi-objective optimization strategy for the optimal control scheme of pumped hydropower systems under successive load rejections," *Appl. Energy*, vol. 261, Mar. 2020, Art. no. 114474.
[13] H. Fang, L. Chen, and Z. Shen, "Application of an improved PSO algorithm to optimal tuning of PID gains for water turbine governor," *Energy Convers. Manage.*, vol. 52, no. 4, pp. 1763–1770, Apr. 2011.
[14] Z. Chen, Y. Yuan, X. Yuan, Y. Huang, X. Li, and W. Li, "Application of multi-objective controller to optimal tuning of PID gains for a hydraulic turbine regulating system using adaptive grid particle swam optimization," *ISA Trans.*, vol. 56, pp. 173–187, May 2015.
[15] C. Jiang, Y. Ma, and C. Wang, "PID controller parameters optimization of hydro-turbine governing systems using deterministic-chaotic-mutation evolutionary programming (DCMEP)," *Energy Convers. Manage.*, vol. 47, nos. 9–10, pp. 1222–1230, Jun. 2006.
[16] R. Zhang, D. Chen, and X. Ma, "Nonlinear predictive control of a hydropower system model," *Entropy*, vol. 17, no. 12, pp. 6129–6149, Sep. 2015.
[17] B. Xu, D. Chen, H. Zhang, F. Wang, X. Zhang, and Y. Wu, "Hamiltonian model and dynamic analyses for a hydro-turbine governing system with fractional item and time-lag," *Commun. Nonlinear Sci. Numer. Simul.*, vol. 47, pp. 35–47, Jun. 2017.
[18] T. Takagi and M. Sugeno, "Fuzzy identification of systems and its applications to modeling and control," *IEEE Trans. Syst., Man, Cybern.*, vol. SMC-15, no. 1, pp. 116–132, Jan. 1985.
[19] Q. Gao, X. J. Zeng, G. Feng, Y. Wang, and J. Qiu, "T–S-fuzzy-model-based approximation and controller design for general nonlinear systems," *IEEE Trans. Syst. Man, Cybern. B, Cybern.*, vol. 42, no. 4, pp. 1143–1154, Aug. 2012.
[20] B. Wang, J. Xue, F. Wu, and D. Zhu, "Robust Takagi-Sugeno fuzzy control for fractional order hydro-turbine governing system," *ISA Trans.*, vol. 65, pp. 72–80, Nov. 2016.
[21] B. Wang, J. Xue, F. Wu, and D. Zhu, "Finite time Takagi-Sugeno fuzzy control for hydro-turbine governing system," *J. Vibrat. Control*, vol. 24, no. 5, pp. 1001–1010, Mar. 2018.
[22] M. Saif, "Optimal linear regulator pole-placement by weight selection," *Int. J. Control*, vol. 50, no. 1, pp. 399–414, Jul. 1989.
[23] J. O'Reilly, *Multivariable Control for Industrial Applications*. London, U.K.: Peter Peregrinus, 1987, p. 4.
[24] S. Srinathkumar, *Eigenstructure Control Algorithms*, 1st ed. Stevenage, U.K.: Institution Engineering Technology, 2011, pp. 12–13 and 45-47.
[25] I. Boulkaibet, K. Belarbi, S. Bououden, T. Marwala, and M. Chadli, "A new T-S fuzzy model predictive control for nonlinear processes," *Expert Syst. Appl.*, vol. 88, pp. 132–151, Dec. 2017.
[26] A. K. Barisal, "Comparative performance analysis of teaching learning based optimization for automatic load frequency control of multi-source power systems," *Int. J. Electr. Power Energy Syst.*, vol. 66, pp. 67–77, Mar. 2015.
[27] O. Saleem and F. Abbas, "Nonlinear self-tuning of fractional-order PID speed controller for PMDC motor," in *Proc. 13th Int. Conf. Emerg. Technol. (ICET)*, Dec. 2017, pp. 1–6.
[28] J. V. D. F. Neto, I. S. Abreu, and F. N. D. Silva, "Neural–genetic synthesis for state-space controllers based on linear quadratic regulator design for eigenstructure assignment," *IEEE Trans. Syst. Man, Cybern. B, Cybern.*, vol. 40, no. 2, pp. 266–285, Apr. 2010.
[29] A. Douik, L. Hend, and H. Messaoud, "Optimised eigenstructure assignment by ant system and LQR approaches," *IJCSA*, vol. 5, no. 4 pp. 45–56, 2008.
[30] Y. Xu, C. Li, Z. Wang, N. Zhang, and B. Peng, "Load frequency control of a novel renewable energy integrated micro-grid containing pumped hydropower energy storage," *IEEE Access*, vol. 6, pp. 29067–29077, 2018.

YIDONG ZOU received the B.S. degree in energy and power engineering from the Hebei University of Engineering, Handan, China, in 2019. He is currently pursuing the M.S. degree in power engineering from the Kunming University of Science and Technology. His research interests include control theory, system identification, and fault diagnosis of hydroelectric units.

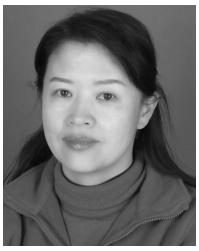

JING QIAN received the B.S. degree in power system and automation from the Huazhong University of Science and Technology, Wuhan, China, in 1989, and the M.S. degree in power system and automation from Sichuan University, in 2000. She is currently a Professor with the Faulty of Metallurgical and Energy Engineering, Kunming University of Science and Technology. Her research interests include stability control of generator set and control of microgrids.

YUN ZENG received the B.S. degree from the Kunming University of Science and Technology, in 1985, and the M.S. and Ph.D. degrees from Hohai University, in 1994 and 2008, respectively. He is currently a Professor and Ph.D. Supervisor with the Kunming University of Science and Technology. His research interest includes the dynamic theory of hydro turbine generating units control and its application.

YAQING GUO received the B.S. degree in engineering management from the Hubei University of Arts and Science, Xiangyang, China, in 2016. She is currently pursuing the M.S. degree in power engineering from the Kunming University of Science and Technology. Her research interests include wind turbine control and stability and economic operation of water turbine generator.

MENGYUN WU received the B.S. degree in new energy science and engineering from Hohai University, Nanjing, China, in 2019. She is currently pursuing the M.Sc. degree in power engineering from the Kunming University of Science and Technology. Her research interest includes the stability and control of hydroelectric generating units.

FANGFANG WANG received the B.S. and M.S. degrees from the Kunming University of Science and Technology, in 2016 and 2019, respectively, where she is currently pursuing the Ph.D. degree. Her research interest includes control and optimization of hydroelectric generating units.

HONG MEI received the B.S. degree in power system and automation from Yunan Polytechnic University, Kunming, China, in 1998, and the M.S. degree in computer science from the Kunming University of Science and Technology, in 2006. He is a Vice-Professor with the Kunming University of Science and Technology. His research interest includes automation of electric power system and virtual reality technology.